Ethylene Glycol Electrooxidation on Smooth and Nanostructured Pd Electrodes in Alkaline Media

Claudio Bianchini, Pei Kang Shen, Francesco Vizza, Lianqin Q. Wang, Valentina Bambagioni, Manuela Bevilacqua, Jonathan Filippi, Andrea Marchionni

Fuel Cells

Ethylene Glycol Electrooxidation on Smooth and Nanostructured Pd Electrodes in Alkaline Media

Journal:	*Fuel Cells*
Manuscript ID:	fuce.200900120.R2
Wiley - Manuscript type:	Original Research Paper
Date Submitted by the Author:	23-Nov-2009
Complete List of Authors:	Bianchini, Claudio; CNR, ICCOM Shen, Pei Kang; Sun Yat-Sen University, School of Physics and Engineering Vizza, Francesco; CNR, ICCOM Q. Wang, Lianqin; Sun Yat-Sen University, School of Physics and Engineering Bambagioni, Valentina; CNR, ICCOM Bevilacqua, Manuela; CNR, ICCOM Filippi, Jonathan; CNR, ICCOM Marchionni, Andrea; CNR, ICCOM
Keywords:	Ethylene glycol electro-oxidation, Electrocatalyst, Pd electrocatalysts, In situ spectroelectrochemical FTIR studies, Cyclic voltammetry

Ethylene Glycol Electrooxidation on Smooth and Nanostructured Pd Electrodes in Alkaline Media

V. Bambagioni[1], M. Bevilacqua[1], C. Bianchini[1*], J. Filippi[1], A. Marchionni[1], F.Vizza[1*], L. Q. Wang[2], P. K. Shen[2*]

[1] Istituto di Chimica dei Composti Organometallici (ICCOM-CNR), Via Madonna del Piano 10, 50019 Sesto Fiorentino, Italy
[2] The State Key Laboratory of Optoelectronic Materials and Technologies, School of Physics and Engineering, Sun Yat-Sen University, Guangzhou 510275, P.R. China

[*] Corresponding authors. Tel.: +39 0555225280; fax: +39 0555225203.
E-mail address: claudio.bianchini@iccom.cnr.it (C. Bianchini); francesco.vizza@iccom.cnr.it (F. Vizza); stsspk@mail.sysu.edu.cn (P. K. Shen)

Abstract

The electrooxidation of ethylene glycol (EG) has been studied either *in situ* on a smooth Pd electrode by FTIR spectroscopy or on nanostructured Pd-based catalysts by cyclic voltammetry. The electrooxidation on the Pd electrode is dramatically influenced by the pH. Below pH 12, CO_2 is formed and detected in the thin layer by FTIR, while at higher pH values glycolate, carbonate and oxalate are formed almost simultaneously at a potential of ca. 0.4 V *vs.* RHE. Above 0.9 V glycolate is oxidized to oxalate and carbonate. The nanostructured electrocatalysts Pd-(Ni-Zn)/C, Pd-(Ni-Zn-P)/C and Pd/C are much more active than the smooth Pd electrode (up to 3300 A $g(Pd)^{-1}$) and give different distributions of the oxidation products. Pd/C is the most selective catalyst yielding glycolate, while mixtures of glycolate (major > 60%), oxalate and carbonate are obtained with Pd-(Ni-Zn)/C or Pd-(Ni-Zn-P)/C. Carbonate is produced by oxidation of both glycolate (major contribution) and oxalate, while the major part of oxalate seems to be produced by the direct oxidation of EG.

Keywords: Ethylene glycol electro-oxidation, Pd electrocatalysts, *In situ* spectroelectrochemical FTIR studies, Cyclic voltammetry

1 Introduction

The electrooxidation of ethylene glycol (EG) on different types of electrodes has been intensely studied over the last 25 years [1-16], largely due to the fact that this diol can be an effective fuel in direct fuel cells in both alkaline and acidic media [17-21]. The interest in EG as an electrochemical fuel has been recently enhanced, because it may be produced from abundant and renewable resources such as cellulose [22]. However, despite some promising achievements [17-21,23], direct ethylene glycol fuel cells (DEGFCs) are still a laboratory device that are not commercially available. This unavailability is largely due to a lack of active and stable anode catalysts, generally based on platinum and platinum alloys, and also to the scarcity of suitable electrolytes for the alkaline environment. Indeed, the alkaline environment offers a number of advantages over the acidic one for alcohol oxidation (see list below) [24,25] but traditional alkaline fuel cells (AFCs) with a liquid electrolyte, suffer some insurmountable problems for an effective application (for instance, membrane carbonation).

- Usability of both noble and non-noble metals to manufacture the electrocatalysts.
- Improved kinetics at both cathode and anode, in particular low anodic over-voltages for alcohol oxidation.
- Alcohol cross-over from anode compartment to cathode compartment reduced by electro-osmotic drag of hydrate hydroxyl ions.
- Easier water management as water is formed at the anode side where an aqueous solution already exists, while the electro-osmotic drag transports water away from the cathode preventing its flooding.
- Reduced risk of corrosion of the materials, including catalysts and carbons.
- Reduced adsorption of spectator ions that might limit electrocatalysis.

The recent development of efficient and chemically stable anion-exchange membranes (AEMs) [27-39] can address the electrolyte issue in DEGFCs as well as contribute to design a new generation of alcohol oxidation electrocatalysts. For example, Pd may effectively replace Pt in alkaline media [25,38-40] where also non-noble metals are sufficiently stable for electrochemical applications. Therefore, it is likely that Pd may be diluted with

non-noble metals to prepare smart catalytic architectures that are capable of functioning as anode electrodes for the rapid and stable oxidation of alcohols. ~~This would decrease the cost of the membrane electrode assemblies (MEAs), thus favouring the commercial viability of DEGFC stacks.~~

Understanding the mechanism of EG electrooxidation on Pd-based electrocatalysts is therefore an important issue for the development of effective DEGFC anodes. Unlike Pt-based electrodes [1-4,7-12,14], a limited number of studies of the electrocatalysis of EG oxidation on Pd-based electrodes has been carried out so far [5,6,13,15,16,20] and no *in situ* experiment has been ever reported. Aimed at filling this gap, we report here a study of the electrooxidation of EG on different types of Pd electrodes. A smooth Pd metal electrode was used for an *in situ* FTIR electrospectroscopy analysis of EG oxidation at different pH values, while cyclic voltammetry (CV) studies have been performed using the nanostructured catalysts Pd-(Ni-Zn)/C and Pd-(Ni-Zn-P)/C. These electrocatalysts, obtained by a redox transmetalation process involving the spontaneous deposition of palladium onto Ni-Zn alloys supported on Vulcan XC-72 [40], have already shown remarkable activity for the oxidation of ethanol in both passive and active fuel cells [38,39]. For comparative purposes, we have investigated also the EG electrooxidation on a nanostructured Pd/C catalyst prepared by chemical reduction of H_2PdCl_4 adsorbed onto Vulcan XC-72 [40].

2 Experimental

2.1 Materials and product analysis

All manipulations, except as stated otherwise, were routinely performed under argon or nitrogen atmosphere. Aqueous solutions were freshly prepared with doubly distilled-deionized water. The electrocatalysts Pd-(Ni-Zn)/C, Pd-(Ni-Zn-P)/C and Pd/C were prepared as previously described [40] (C = Vulcan XC-72). ICP-AES analysis (wt%) for Pd-(Ni-Zn)/C: Pd 6.4, Ni 9.7, Zn 2.6; for Pd-(Ni-Zn-P)/C: Pd 4.73, Ni 7.45, Zn 0.43; for Pd/C: Pd 5.2.

The qualitative/quantitative analysis of the CV cell exhausts was obtained by $^{13}C\{^1H\}$ NMR spectroscopy using a Bruker Avance DRX-400 instrument with the chemical shifts relative to external TMS. The calibration curves for the quantitative analysis were obtained using authentic samples of the various products in the appropriate range of concentrations, using 1,4-dioxane as internal standard. Ionic chromatography (IC) was also used to identify and quantify the oxidation products (Metrohm 761 Compact instrument equipped with a Metrosep Organic Acids column).

2.2 Electrochemical measurements

2.2.1 Ink preparation for the CV study

A portion of each catalyst (about 45 mg) was introduced into a 5 mL high-density polyethylene container together with 1.01 g of water, 65 mg of KOH (99.99% Sigma-Aldrich), 0.50 g of absolute ethanol (99.8% Fluka) and 0.37 g of 5% Nafion® ion-exchange resin in alcohol solution (Sigma-Aldrich). The resulting suspension was sonicated for 30 min with a Branson 3200 bath. Each suspension was freshly prepared just before carrying out the experiment scheduled. The metal loading on each glassy carbon electrode (*vide infra*) was determined by weighting the amount of ink deposited on the glassy carbon disk.

2.2.2 Apparatus for cyclic voltammetry studies

The cell used for the cyclic voltammetry (CV) experiments was a Kelef cylinder with a 7.2 mm inner diameter and a 50 mm outer diameter [40]. The inner volume of the cell was about 1 mL. The working electrode, Glassy Carbon (Sigradur® G) (0.867 cm^2), covered by the catalyst, was housed in a cavity at the top end of the cylinder, and the counter electrode was a gold disc placed at the bottom end. The solution contained in a Pyrex flask was previously purged by bubbling N_2 and then flushed into the cell by a pressure as low as 0.3 bar of N_2. The miniaturized reference electrode, $Ag/AgCl/KCl_{sat}$, was placed on the outlet tubing. This design allows one to avoid contamination and at the same time is sufficiently close to the working electrode to reduce the uncompensated resistance. All CV studies were carried out using a Parstat 2277 potentiostat-galvanostat (Princeton Applied Research).

2.3 *In situ* FTIR spectroelectrochemical study

A cell equipped with a CaF_2 window was used for the electrochemical and *in situ* FTIR measurements. The working electrode was a palladium electrode with a 6 mm diameter. A platinum foil and an Hg/HgO electrode were used as the counter and reference electrode, respectively. The electrochemical measurements were performed on a 263A potentialstat/galvanostrat (EG&G-PARC, USA), connected to the FTIR spectrometer

(Nicolet 5700 with DTGS detector, Thermo Electron Corporation, USA). The measurements were carried out at 25 °C. The EG concentration was fixed at 1 M. Electrolytes with different NaOH concentrations were used to investigate the pH effect on the EG electrooxidation. When necessary, $NaClO_4$ was added to the NaOH solutions to ensure a constant ionic strength. All solutions were purged with nitrogen prior to use. Prior to each experiment, the palladium electrode was polished with alumina powder, followed by a supersonic rinsing in pure water and a potential cycling in 0.1 M $HClO_4$ at 0.1 V s^{-1} between 0.242 V and 1.2 V *vs.* SCE with a reductive final potential. Afterwards, the palladium electrode was immersed into the electrochemical cell. During the *in situ* FTIR spectroelectrochemical experiments, the electrode was pressed against the CaF_2 window to form a thin layer solution. Each infrared spectrum was recorded from 128 interferograms at the resolution of 4 cm^{-1}. The reference spectrum (R_{ref}) was collected at 0 V *vs.* RHE. The electrode potentials were increased by 0.1 V intervals from the reference potential up to 1.2 V. The equilibrium at each potential was achieved in 5 s before the collection of the sample spectra (R_s). Each final spectrum was reported using Eq. (1). Accordingly, the negative bands represent the species produced and the positive bands the species consumed.

$$\frac{\Delta R}{R} = \frac{R_s - R_{ref}}{R_{ref}} \quad (1)$$

All the potentials in the figures were quoted with respect to the reversible hydrogen electrode (RHE).

3 Results and Discussion

3.1 *In situ* FTIR study

The influence of the pH on the EG electrooxidation on a smooth Pd electrode was investigated by CV using 1 M EG solutions with different NaOH concentrations but comparable ionic strengths (Figure 1). From a perusal of this figure one may readily realize that the catalytic activity of the Pd electrode decreases by decreasing the pH, until it almost disappears at pH 12. No activity was detected in neutral or acidic media. This finding has been already observed for the oxidation of ethanol on Pd electrodes and rationalized both experimentally and theoretically [41,42]. In particular, DFT calculations suggest that the dehydrogenation of ethanol to acetaldehyde requires a high OH_{ads} coverage of the Pd surface [42].

Figure 1 here

FTIR spectroscopy was used to gain insight into the mechanism of EG electrooxidation on Pd at different pH values (Figure 2). At NaOH concentrations ≥ 1 M, the stretching bands of the glycolate ion at 1580 cm^{-1} (C=O) and 1070 cm^{-1} (C-O) were clearly observed together with lower-intensity bands at 1410 and 1310 cm^{-1} assignable to carbonate and oxalate, respectively (Figures 2c-d) [4]. The stretch of the oxalate group expected at 1600 cm^{-1} is likely masked by the band of glycolate. Consistent with the CV study, increasing the pH decreases the onset potential of EG oxidation. At NaOH concentrations ≤ 1 M, the characteristic band of CO_2 at 2343 cm^{-1} was observed already at 0.7 V [3,4]. The detection of CO_2 suggests that the pH drops in the thin layer due to the consumption of OH^- groups (*vide infra*). No band due to CO was detected at any pH or potential. In this respect, it is worth recalling that the IR detection of CO_{ads} is particularly difficult in an alkaline electrolyte [43], especially at the very low concentrations expected in the present case. The occurrence of C-C bond breaking of an alcohol with formation of CO_2 at relatively low pH values is in line with previous reports according to which a high OH coverage of the Pd surface is essential for releasing carboxylate products by Pd-acyl/OH coupling [38-41].

Figure 3 shows the potential dependence of the integrated intensities of the glycolate C=O (A) and C-O (B) bands at 1580 and 1070 cm^{-1}, respectively, in the thin layer solution. The onset potential of EG oxidation apparently decreases by increasing the NaOH concentration and the intensity of either band reaches a maximum at ca. 0.9 V. Above this potential, however, the intensities of these two bands diverge, which can be attributed to an increase of the oxalate band at 1600 cm^{-1} enhancing the intensity of the glycolate band (see also the increase in intensity of the band at 1310 cm^{-1}).

Figure 2 here

Figure 3 here

Overall, the electrooxidation of EG on Pd does not diverge substantially from that on Pt [1-4,7-12,14]: glycolate, oxalate and carbonate seem to form at the same potential with an increase of oxalate and carbonate

formation at the expense of glycolate above 0.9 V. What really distinguishes Pd from Pt is the higher electrochemical activity of the former metal in alkaline media.

The lack of reports in the relevant literature dealing with *in situ* FTIR studies of EG electrooxidation on Pd does not allow one to make a direct comparison with the present results. However, it is worthwhile to discuss some studies of EG oxidation on Pt electrodes in alkaline media. In view of EMIR spectroscopy, Kardigan et al. have concluded that the adsorption of EG at a Pt electrode is dissociative at any pH with formation of CO_{ads} [2], which contrasts with the behavior of Pd-based catalysts (vide infra). Besides confirming the presence of linearly bonded CO at high pH values, a SNIFTIR study by Christensen and Hamnett has shown the formation of glycolate, oxalate and carbonate upon oxidation of EG on Pt in alkaline media [4]. Based on the potential window at which these products were detected as well as the EG concentration, it was suggested that glycolate and carbonate are produced from the same intermediate (e. g. Pt-CH(OH)CH_2OH), while oxalate is obtained by oxidation of desorbed glycolate. Likewise, a following SPAIR study of EG electrooxidation on Pt/C, PtPd/C, PtBi/C and PtBiPd/C electrodes has provided evidence that oxalate is not a primary product of EG oxidation but it comes from adsorption and oxidation of glycolate [20]. Traces of glyoxylic acid and formic acid were also detected by HPLC. Coutanceau et al. have found that the addition of Pd to Pt-base catalysts reduces the amount of strongly adsorbed carbonyl species at Pt, leading to higher current densities by virtue of the low propensity of Pd to cleave C-C bonds [20]. It was also proposed that Bi exerts a beneficial effect on the onset potential of EG electrooxidation as well as on the catalyst stability by virtue of the greater propensity of Bi to adsorb and activate hydroxyl groups as compared to Pd.

3.2 CV studies

The electrochemical activity of the nanostructured catalysts Pd-(Ni-Zn)/C, Pd-(Ni-Zn-P)/C and Pd/C for EG oxidation was investigated by CV at room temperature. A preliminary study was carried out to find suitable conditions in terms of catalyst loading on the electrode and of KOH concentration. For all catalysts, Pd loadings varying from 24 to 28 μg cm^{-2}, corresponding to 18-20 mg of ink, gave the highest current density values in 2 M KOH at a scan rate of 50 mV s^{-}1. A series of cyclic voltammograms, recorded at KOH concentrations spanning from 0.01 to 4 M, showed the generation of the highest current densities in the range 1.5-2 M KOH. The following electrochemical studies in half cells were carried out using a 2 M KOH solution, a proper condition to keep a relatively high OH^- concentration during the CV and chronoptentiometric experiments. Indeed, the oxidation of EG in alkaline media consumes OH^- groups, irrespective of the oxidation level of the substrate (glycolate, oxalate or carbonate, Eqs. (1)-(3)).

$$(CH_2OH)_2 + 5\ OH^- \rightarrow CH_2(OH)COO^- + 4\ H_2O + 4\ e^- \quad (1)$$
$$(CH_2OH)_2 + 10\ OH^- \rightarrow (CO_2)_2^{2-} + 8\ H_2O + 8\ e^- \quad (2)$$
$$(CH_2OH)_2 + 14\ OH^- \rightarrow 2\ CO_3^{2-} + 10\ H_2O + 12\ e^- \quad (3)$$

The EG concentration was fixed at 5 wt% as this value has been found appropriate for DEGFCs with AEMs [44]. On the other hand, a previous CV study of EG electrooxidation on a smooth Pd electrode has demonstrated that the current densities are practically independent on the EG concentration but proportional to the OH^- concentration with a reaction order of ca. 1 [5].

In conclusion, all the CV measurements reported below were performed at a sweep rate of 50 mV s^{-1} in deoxygenated 5 wt% EG, 2 M KOH solutions and electrodes containing a Pd loading between 24 and 28 μg cm^{-2}.

Figure 4 shows the cyclic voltammograms of the EG oxidation reaction on Pd/C, Pd-(Ni-Zn-P)/C and Pd-(Ni-Zn)/C electrodes.

Figure 4 here

Relevant electrochemical parameters such as the peak current density (J_p), the specific peak current density (Sa_p), the forward anodic peak potential (V_p), the onset oxidation potential (V_{onset}) and the Tafel slopes, together with the electronic transfer coefficient α, are given in Table 1. The three catalysts show high activity for the EG oxidation reaction with onset potentials at ca. 0.4 V *vs.* RHE and specific current densities higher than 3 mA μgPd^{-1} for Pd-(Ni-Zn)/C and Pd/C. Accordingly, Pd-(Ni-Zn)/C, Pd-(Ni-Zn-P)/C and Pd/C can be classified amongst the best performing electrocatalysts ever reported for EG oxidation. As expected, the oxidation of EG starts at the potential corresponding to the coverage of the electrode surface by OH groups [5,15,16,38,40]. A specific CV study of the Pd-(Ni-Zn)/C, Pd-(Ni-Zn-P)/C and Pd/C electrodes in 2 M KOH solution without EG has been previously reported [40] and the corresponding CVs are also shown in Figure 7.

As shown by the traces in Figure 4, the three electrocatalysts are characterized by rather similar activities with Pd-(Ni-Zn)/C being slightly more active than Pd/C, especially in terms of forward and backward anodic

peak potentials. Since we observed for all catalysts a slow but constant decrease of the peak back current with increasing the anodic limit (from 0.9 to 1.6 V), the backward scan peak can be associated to the oxidation of freshly chemisorbed EG. In fact, previous CV studies of ethanol oxidation on Pd have shown that the decrease in current at high voltages is mainly due to the formation of a PdO layer, which blocks the adsorption of the substrate [41]. The electrocatalytic activity is restored in the negative-going sweep once the potential reaches the value at which PdO is reduced to Pd. On the other hand, one cannot rule out that a contribution to the current decrease may be due to mass transfer phenomena as well as the instantaneous shortage of OH^- groups in the thin layer. In fact, adsorbed OH species are required to release the carboxylic acid upon coupling with Pd-acyl species as shown in Scheme 1 [39]. Previous studies of ethanol oxidation on Pd-(Ni-Zn)/C and Pd-(Ni-Zn-P)/C [40] have unambiguously shown that the Ni-based supports, though able to oxidise ethanol in alkaline media, are not directly involved in the ethanol oxidation reaction occurring at the largely negative potentials of the Pd-containing electrocatalysts. It has been proposed that Ni increases the amount of OH_{ads} groups on the catalyst surface, which would favour the formation of the carboxylic acid by coupling with $acyl_{ads}$ species [25,40]

Table 1 here

Scheme 1 here

Tafel plots for the EG oxidation reaction on the Pd-(Ni-Zn)/C, Pd-(Ni-Zn-P)/C and Pd/C electrodes were obtained at a scan rate of 5 mV s^{-1} in the potential interval from 0.3 to 0.5 V (2 M KOH, 5 wt% EG). The values for the Tafel slopes and of the α coefficients (Table 1) are comparable with each other as well as with those reported for nanostructured Pd electrocatalysts supported on the same carbon black, also promoted by metal oxides [13,15,38,40]. These values are higher than those reported for a smooth Pd electrode (120 mV dec^{-1}) [5], most likely due to the porous high surface area of the present electrodes [38,15]. The Tafel slopes indicate a similar reaction mechanism for the three electrocatalysts, while the α parameter of ca. 0.3 is consistent with an electrochemical rate limiting step for the EG oxidation reaction.

For all electrodes, the anodic peak current density for EG oxidation was plotted against the square-root of the scan rate (Figure 5). A linear relationship, typical of an electrochemical reaction under diffusion control, was found for the Pd-(Ni-Zn)/C and Pd-(Ni-Zn-P)/C electrodes. In contrast, a slightly parabolic curve was observed for the Pd/C electrode, which suggests a reaction controlled by the activation polarization. As previously reported for the oxidation of ethanol on a similar Pd/C electrode [40], this effect can be related to the very low number of catalytically active sites on the electrode surface due to the low Pd dispersion: just by increasing the metal loading is the reaction controlled by substrate diffusion [40].

The performance stability of the three electrocatalysts for EG oxidation was investigated by chronopotentiometry. Steady state measurements, carried out with a constant current density polarization of 3.46 mA cm^{-2} showed a negligible potential oscillation for 2 hours, indicative of no strongly adsorbed species on the catalyst surface. Notably, the selective formation of glycolate with trace amounts of oxalate and carbonate (Eq. (1)) was determined by ionic chromatography/^{13}C NMR analysis of the chronopotentiometric exhausts produced by Pd/C as electrocatalyst. Pd-(Ni-Zn)/C, Pd-(Ni-Zn-P)/C gave a different product distribution. On both electrocatalysts EG was prevalently converted to glycolate (57-63%) but appreciable amounts of oxalate (35-30%) and carbonate (8-7%) were also formed, revealing a different chemoselectivity of EG oxidation of the nanostructured catalysts promoted by the Ni-Zn and Ni-Zn-P alloys as compared to plain Pd/C. In no case were glyoxaldehyde or its hemiacetal detected by NMR spectroscopy on the cell exhausts.

The different product distribution provided by Pd-(Ni-Zn)/C and Pd-(Ni-Zn-P)/C as compared to Pd/C seems to be inconsistent with a similar reaction mechanism for the three catalysts, as suggested by the Tafel slopes. A clear-cut explanation of this phenomenon is not available at this stage: the rate-determining step seems to be electrochemical in nature but it has not been identified among the several oxidation steps occurring for EG oxidation on the electrode surfaces. On the other hand, a precise quantification of the oxidation products may be inaccurate due to the little EG conversion in the chronopotentiometric experiments.

Figure 5 here

Overall, the electrooxidation of EG on Pd-(Ni-Zn)/C, Pd-(Ni-Zn-P)/C and Pd/C resembles that of ethanol oxidation on the same electrodes that selectively yields potassium acetate [39,40]. Unlike ethanol, however, EG contains two hydroxyl groups so that in alkaline media at least three carboxylate products (glycolate, glyoxylate and oxalate) plus formate and carbonate may be obtained upon electrooxidation (Scheme 2). This scheme illustrates the overall electrochemical oxidation of EG in alkaline media as inferred from a perusal of the literature [3,4,7,9,11,12,14,20] as well as the present results. The scheme includes all the species that have been either isolated (boxes) or detected *in situ* (circles).

Scheme 2 here

In an attempt to gain insight into the EG electroxidation on the present nanostructured Pd catalysts, independent CV experiments have been carried out using solutions of potassium glycolate, potassium glyoxylate and potassium oxalate as anolytes.

The cyclic voltammograms of glycolic acid and glyoxylic acid oxidation on Pd-(Ni-Zn)/C, Pd-(Ni-Zn-P)/C or Pd/C in 2 M KOH are shown in Figure 6.

Figure 6 here

The glycolate ion is much more difficult to oxidize on Pd than EG as shown by the corresponding Sa_p values which are one order of magnitude lower than those observed for EG (Figure 6A). Slightly higher current densities are produced by glyoxylate (Figure 6B) which can be an intermediate along the conversion of EG and glycolate to oxalate (Scheme 2). The aldehyde group is oxidized on Pd at a more negative potential than the alcohol group as shown also by the shoulder at ca. 0.85 V in Fig. 6 (right) corresponding to the oxidation of the glycolate formed upon disproportionation of the aldehyde in alkaline media. Notwithstanding the low current density observed, there is little doubt that glycolate can be oxidized to oxalate on Pd. On the other hand, just the very low current densities provided by glycolate oxidation on Pd-(Ni-Zn)/C and Pd-(Ni-Zn-P)/C and the fact that both electrocatalysts yield relatively large amounts of oxalate and carbonate indicate that the oxidation of EG on these catalysts proceeds by parallel routes with path c prevailing over paths a-b for oxalate production (Scheme 3).

Scheme 3 here

In an attempt to understand whether oxalate is oxidized to CO_2 on the present nanostructured Pd-based electrocatalysts, a CV study has been carried out on an alkaline solution of potassium oxalate. The corresponding cyclic voltammograms are given in Figure 7 that also shows those recorded on KOH solutions with no substrate. Upon addition of oxalic acid to the latter solutions, a significant decrease of the peak associated to PdO reduction in the reverse scan at ca. 0.65 V is observed together with an oxidation peak at 0.47 V featured by a very low specific current. Accordingly, one may conclude that the carbonate formed upon electrooxidation of EG on Pd-(Ni-Zn)/C and Pd-(Ni-Zn-P)/C is prevalently obtained from glycolate with a very minor contribution from oxalate.

Figure 7 here

3 Conclusions

The electrooxidation of EG on Pd is dramatically influenced by the pH. Below pH 12, CO_2 is formed and detected in the thin layer by FTIR, while at higher pH values glycolate, carbonate and oxalate are formed almost simultaneously at a potential of ca. 0.4 V *vs.* RHE. Above 0.9 V glycolate is oxidized to oxalate and carbonate.

The electrodes with the nanostructured catalysts Pd-(Ni-Zn)/C, Pd-(Ni-Zn-P)/C and Pd/C are much more active than the smooth Pd electrode and give different distributions of the oxidation products. Pd/C is the most selective electrocatalyst yielding glycolate, while mixtures of glycolate (major > 60%), oxalate and carbonate are obtained with Pd-(Ni-Zn)/C or Pd-(Ni-Zn-P)/C. Carbonate is produced by oxidation of both glycolate (major contribution) and oxalate, while the major part of oxalate seems to be produced by the direct oxidation of EG (Scheme 3, route c). The Ni-Zn and Ni-Zn-P phases supporting the Pd clusters might favour the chelating adsorption of EG, leading to its direct oxidation to oxalate, by virtue of the oxophylic nature of both Ni and Zn [40].

In light of the results obtained in this work, current studies in our laboratories are aimed at developing MEAs with Pd-based anode electrodes and anion-exchange membranes for both passive and active DEGFCs.

Acknowledgments

We acknowledge the financial support from the European Commission (Network of Excellence IDECAT, contract n. NMP3-CT-2005-011730), Regione Toscana (Progetto CESARE) and the MIUR (Italy) for the PRIN 2007 project 200775CREC-004. Thanks are also due to the Guangdong Sci. & Tech. Key Projects (2007A010700001, 2007B090400032) and Guangzhou Sci. & Tech. Key Projects (2007Z1-D0051SKT[2007]17-11) for financial support.

References

[1] W. Hauffe, J. Heitbaum, *Electrochim. Acta* **1978**, *23*, 299.
[2] F. Hahn, B. Beden, F. Kardigan, C. Lamy, *J. Electroanal. Chem.* **1987**, *216*, 169.
[3] L.-W. H. Leung, M. J. Weaver, *J. Phys. Chem* **1988**, *92*, 4019.
[4] P. A. Christensen, A. Hamnett, *J. Electroanal. Chem.* **1989**, *260*, 347.
[5] N. Dalbay, F. Kardigan, *J. Electroanal. Chem.* **1990**, *296*, 559.
[6] R. Pattabiram, *Appl. Catal. A. General* **1997**, *153*, 9.
[7] B. Wieland, J. P. Lancaster, C. S. Hoaglund, P. Holota, W. J. Tornquist, *Lamgmuir* **1996**, *12*, 2594.
[8] M. J. Gonzàlez, C. T. Hable, M. S. Wrighton, *J. Phys. Chem. B* **1998**, *102*, 9881.
[9] A. Dailey, J. Shin, C. Korzeniewski, *Electrochim. Acta* **1998**, *44*, 1147.
[10] E. Peled, T. Dudvedani, A. Ahra, *Electrochem. Solid-State Lett.* **2001**, *4*, A38.
[11] R. B. De Lima, V. Paganin, T. Iwasita, W. Vielstich, *Electrochim. Acta* **2003**, *49*, 85.
[12] K. Matsuoka, Y. Iriyama, T. Abe, M. Matsuoka, Z. Ogumi, *Electrochim. Acta* **2001**, *51*, 1085.
[13] Z. Wang, F. Hu, P. K. Shen, *Electrochem. Commun.* **2006**, *8*, 1764.
[14] H. Wang, Z. Jusys, R, J. Behm, *J. Electroanal. Chem.* **2006**, *595*, 23.
[15] P. K. Shen, C. Xu, *Electrochem. Commun.* **2006**, *8*, 184.
[16] C. Xu, Z. Tian, P. K. Shen, S. P. Jiang, *Electrochim. Acta* **2008**, *53*, 2610.
[17] K. Matsuoka, Y. Iriyama, T. Abe, M. Matsuoka, Z. Ogumi, *J. Power Sources* **2005**, *150*, 27.
[18] C. Coutanceau, L. Demarconnay, C. Lamy, J.-M Léger, *J. Power Sources* **2006**, *156*, 14.
[19] V. Livshits, E. Peled, *J. Power Sources* **2006**, *161*, 1187.
[20] L. Demarconnay, S. Brimaud, C. Coutanceau, J.-M- Léger, *J. Electroanal. Chem.* **2007**, *601*, 169.
[21] V. Livshits, M. Philosoph, E. Peled, *J. Power Sources* **2008**, *178*, 687.
[22] N. Ji, T. Zhang, M. Zheng, A. Wang, H. Wang, X. Wang, J. G. Chen, *Angew. Chem. Int. Ed. Engl.* **2008**, *47*, 8510.
[23] C. Cnobloch, D. Gröppel, H. Kohlmüller, D. Kühl, H. Poppa, G. Siemens, *Progr. Batteries & Solar Cells* **1982**, *4* , 225.
[24] J. S. Spendelow, A. Wieckowski, *Phys. Chem. Rev. Phys.* **2007**, *9*, 2654.
[25] C. Bianchini, P. K. Shen, *Chem. Rev.* **2009**, *109*, 4183.
[26] J. R. Varcoe, R. C. T. Slade, E. L. H. Yee, *Chem. Commun.* **2006**, 1428.
[27] J. R. Varcoe, R. C. T. Slade, *Electrochem. Comm.* **2006**, *8*, 839.
[28] J. R. Varcoe, R. C. T. Slade, E. L. H. Yee, D. D. Poynton, D. J. Driscoll, *J. Power Sources* **2007**, *173*, 194.
[29] T. Xu, *J. Membr. Sci.* **2005**, *263*, 1.
[30] J. Fang, P. K. Shen, *J. Membrane Sci.* **2006**, *285*, 317.
[31] H. Hou, G. Sun, R. He, Z. Wu, B. Sun, *J. Power Sources* **2008**, *182*, 95.
[32] K. Scott, E. Yu, G. Vlachogiannopoulos, M. Shivare, N. Duteanu, *J. Power Sources* **2008**, *175*, 452.
[33] E. Hao, K. Scott, *J. Power Sources* **2004**, *137*, 248.
[34] Y. Xiong, Q. L. Liu, A. M. Zhu, S. M. Huang, Q. H. Zeng, *J. Power Sources* **2009**, *186*, 328.
[35] E. Agel, J. Bouet, J. –F. Fauvarque, H. Yassir, *H. Ann. Chim. Sci. Mat.* **2001**, *26*, 59.
[36] H. Bunawaza, Y. Yamazaki, *J. Power Sources* **2008**, *182*, 48.
[37] F. Lu, J. Pan, A. Huang, L. Zhuang, J. T. Lu, *PNAS* **2008**, *105*, 20611.
[38] V. Bambagioni, C. Bianchini, A. Marchionni, J. Filippi, F. Vizza, J. Teddy, P. Serp, M. Zhiani, *J. Power Sources* **2009**, *190*, 241.
[39] V. Bambagioni, C. Bianchini, J. Filippi, A. Marchionni, F. Vizza, P. Bert, A. Tampucci, *Electrochem. Commun.* **2009**, *11*, 1077.
[40] V. Bambagioni, C. Bianchini, J. Filippi, W. Oberhauser, A. Marchionni, F. Vizza, R. Psaro, L. Sordelli, M. L. Foresti, M. Innocenti, *ChemSusChem* **2009**, *2*, 99.
[41] Z. X. Liang, T. S. Zhao, J. B. Xu, L. D. Zhu, *Electrochim. Acta* **2009**, *54*, 2203.
[42] G. F. Cui, S. Q. Song, P. K. Shen, A. Kowal, C. Bianchini, *J. Phys. Chem.* **2009**, 113, 15639.
[43] E. Morallón, A. Rodes, J. L. Vázquez, J. M. Pérez, *J. Electroanal. Chem.* **1995**, *391*, 149.
[44] C. Bianchini, F. Vizza, P. K. Shen, manuscript in preparation.

Tables

Table 1. Selected electrochemical parameters of EG oxidation on Pd-(Ni-Zn)/C, Pd-(Ni-Zn-P)/C and Pd/C electrodes in 2 M KOH.

Catalyst	J_p, mA cm^{-2}	Sa_p mA(μ gPd)$^{-1}$	V_{onset} V	V_p V	Tafel slope mV dec^{-1}
Pd-(Ni-Zn)/C	84.2	3.33	0.37	1.02	205 (α 0.284)
Pd-(Ni-Zn-P)/C	65.5	2.46	0.42	0.95	190 (α 0.307)
Pd/C	84.5	3.15	0.42	0.95	180 (α 0.324)

Figure captions

Figure 1. Cyclic voltammograms on a Pd electrode of the following solutions: (a) 0.01M NaOH + 0.99 M $NaClO_4$ + 1 M EG; (b) 0.1 M NaOH + 0.9 M $NaClO_4$ + 1 M EG; (c) 1 M NaOH + 1 M EG; (d) 2 M NaOH + 1 M EG. Scan rate: 50 mV s^{-1}

Figure 2. *In situ* FTIR spectra obtained under potential step polarization of the following solutions: (a) 0.01 M NaOH + 0.99 M $NaClO_4$ + 1 M EG; (b) 0.1 M NaOH + 0.9 M $NaClO_4$ + 1 M EG; (c) 1 M NaOH + 1 M EG; (d) 2 M NaOH + 1 M EG. Scan number: 128.

Figure 3. (A) Intensity of the band at 1580 cm^{-1} as a function of the polarization potential. (a) 0.01 M NaOH + 0.99 M $NaClO_4$ + 1 M EG; (b) 0.1 M NaOH + 0.9 M $NaClO_4$ + 1 M EG; (c) 1 M NaOH + 1 M EG; (d) 2 M NaOH + 1 M EG. (B) Intensity of the band at 1070 cm^{-1} as a function of the polarization potential. (a) 0.01 M NaOH + 0.99 M $NaClO_4$ + 1 M EG; (b) 0.1 M NaOH + 0.9 M $NaClO_4$ + 1 M EG; (c) 1 M NaOH + 1 M EG; (d) 2 M NaOH + 1 M EG.

Figure 4. Cyclic voltammograms (at the tenth cycle) of EG oxidation on Pd-(Ni-Zn)/C, Pd-(Ni-Zn-P)/C and Pd/C electrodes in 2 M KOH and 5 wt% EG. Scan rate: 50 mV s^{-1}.

Scheme 1. Proposed mechanism for the electrooxidation of EG to glycolate acid on Pd in alkaline media.

Figure 5. Plots of the anodic peak specific current density against the square-root of the scan rate for the oxidation of EG (5 wt%) on Pd-(Ni-Zn)/C, Pd-(Ni-Zn-P)/C and Pd/C in 2 M KOH.

Scheme 2. Overall reaction scheme of EG oxidation on metal electrocatalysyts in alkaline media. Products in boxes have been isolated; products in circles have been detected spectroscopically.

Figure 6. Cyclic voltammograms of (A) glycolic acid (2 wt%) and (B) glyoxylic acid (2 wt%) oxidation on Pd-(Ni-Zn)/C, Pd-(Ni-Zn-P)/C and Pd/C in 2 M KOH. Scan rate: 50 mV s^{-1}.

Scheme 3. Direct and sequential routes for the electrooxidation of EG to oxalic acid.

Figure 7. Cyclic voltammograns of Pd-(Ni-Zn)/C, Pd-(Ni-Zn-P)/C and Pd/C in 2 M KOH or in 2 M KOH +2 wt% oxalic acid. Scan rate: 50 mV s^{-1}.

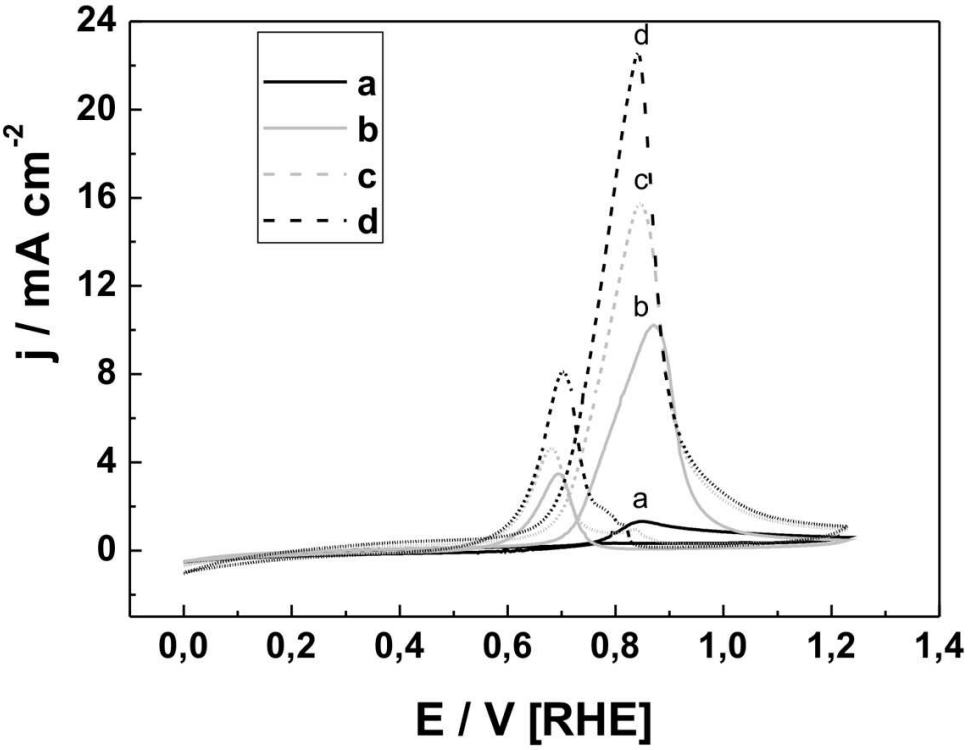

Figure 1. Cyclic voltammograms on a Pd electrode of the following solutions: (a) 0.01M NaOH + 0.99 M NaClO4 + 1 M EG; (b) 0.1 M NaOH + 0.9 M NaClO4 + 1 M EG; (c) 1 M NaOH + 1 M EG; (d) 2 M NaOH + 1 M EG. Scan rate: 50 mV s−1
74x57mm (400 x 400 DPI)

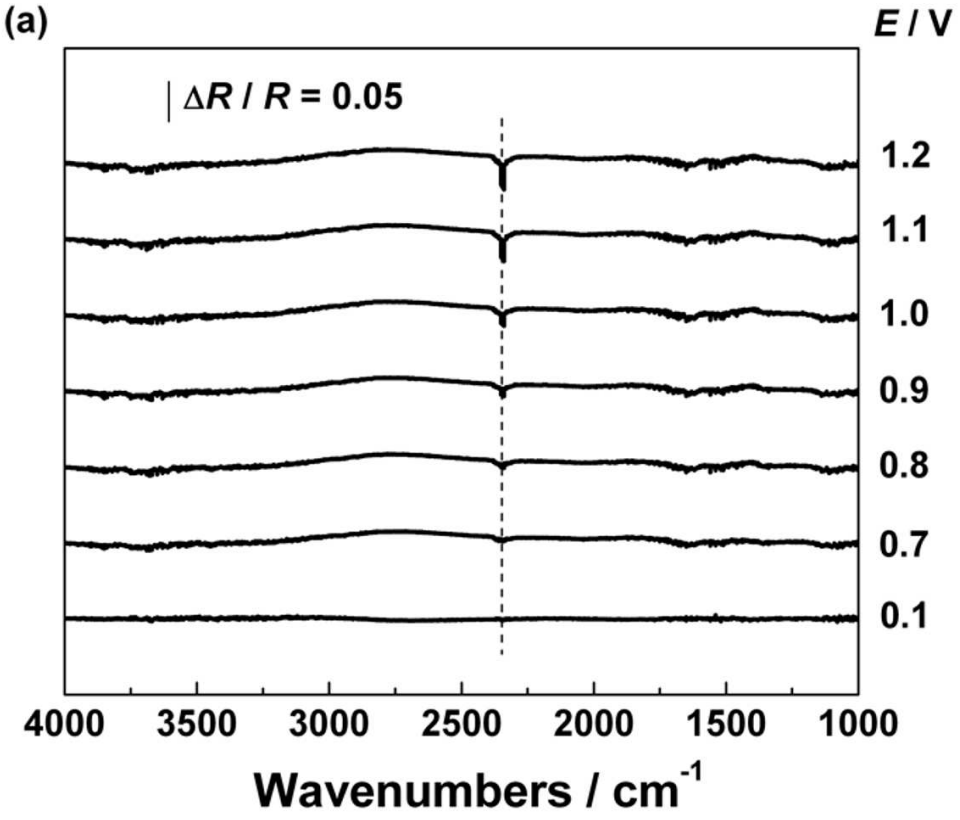

Figure 2. In situ FTIR spectra obtained under potential step polarization of the following solutions: (a) 0.01 M NaOH + 0.99 M NaClO4 + 1 M EG; (b) 0.1 M NaOH + 0.9 M NaClO4 + 1 M EG; (c) 1 M NaOH + 1 M EG; (d) 2 M NaOH + 1 M EG. Scan number: 128.
74x65mm (400 x 400 DPI)

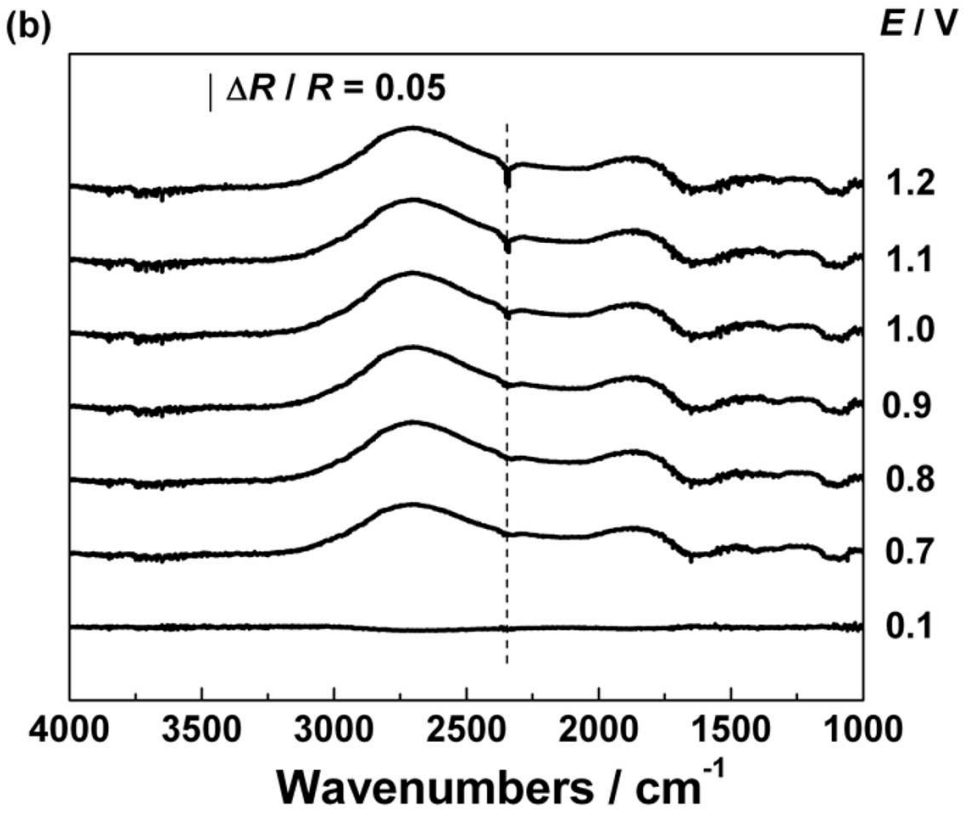

Figure 2. In situ FTIR spectra obtained under potential step polarization of the following solutions: (a) 0.01 M NaOH + 0.99 M NaClO4 + 1 M EG; (b) 0.1 M NaOH + 0.9 M NaClO4 + 1 M EG; (c) 1 M NaOH + 1 M EG; (d) 2 M NaOH + 1 M EG. Scan number: 128.
74x65mm (400 x 400 DPI)

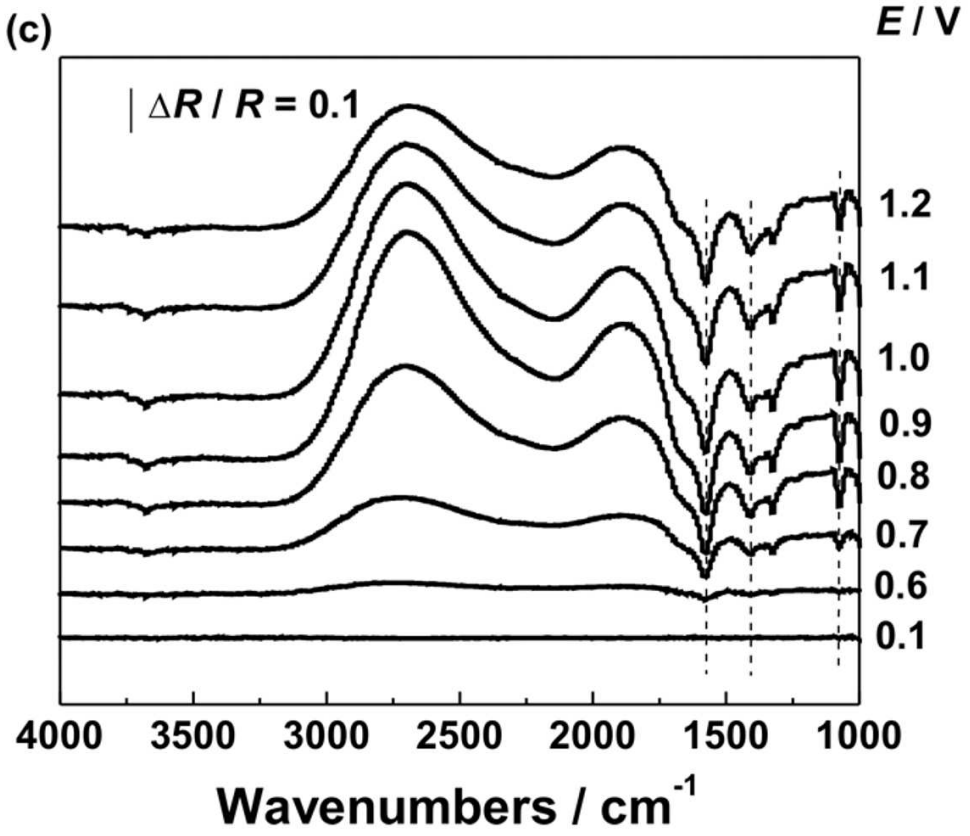

Figure 2. In situ FTIR spectra obtained under potential step polarization of the following solutions: (a) 0.01 M NaOH + 0.99 M NaClO4 + 1 M EG; (b) 0.1 M NaOH + 0.9 M NaClO4 + 1 M EG; (c) 1 M NaOH + 1 M EG; (d) 2 M NaOH + 1 M EG. Scan number: 128.
74x65mm (400 x 400 DPI)

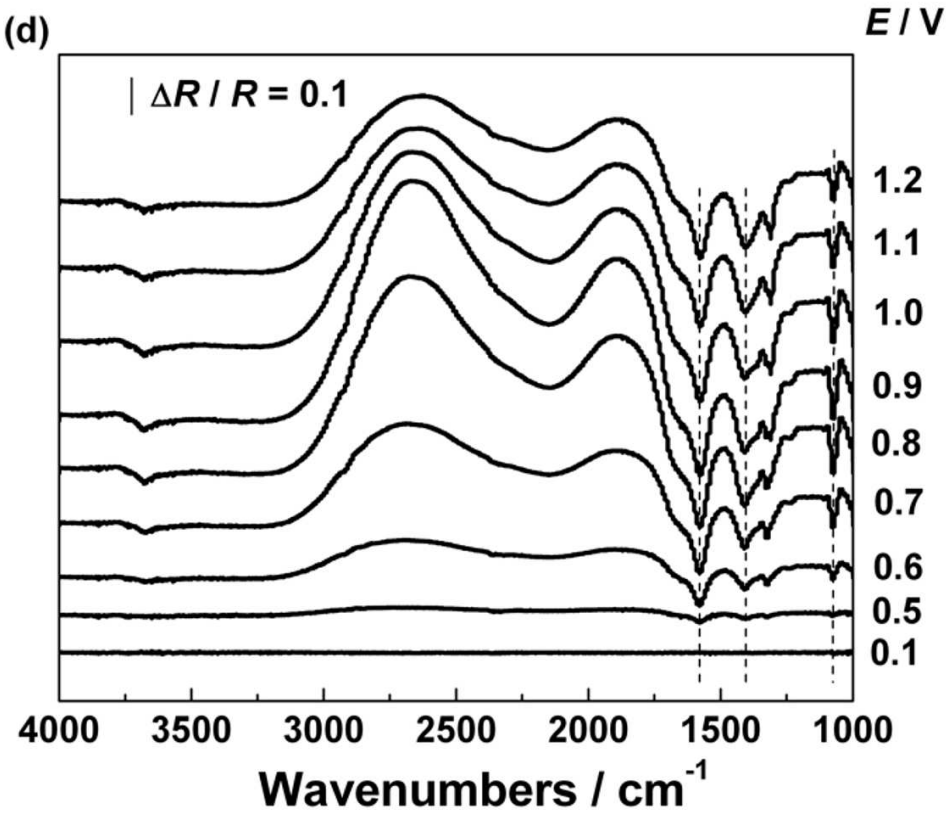

Figure 2. In situ FTIR spectra obtained under potential step polarization of the following solutions: (a) 0.01 M NaOH + 0.99 M NaClO4 + 1 M EG; (b) 0.1 M NaOH + 0.9 M NaClO4 + 1 M EG; (c) 1 M NaOH + 1 M EG; (d) 2 M NaOH + 1 M EG. Scan number: 128.
74x65mm (400 x 400 DPI)

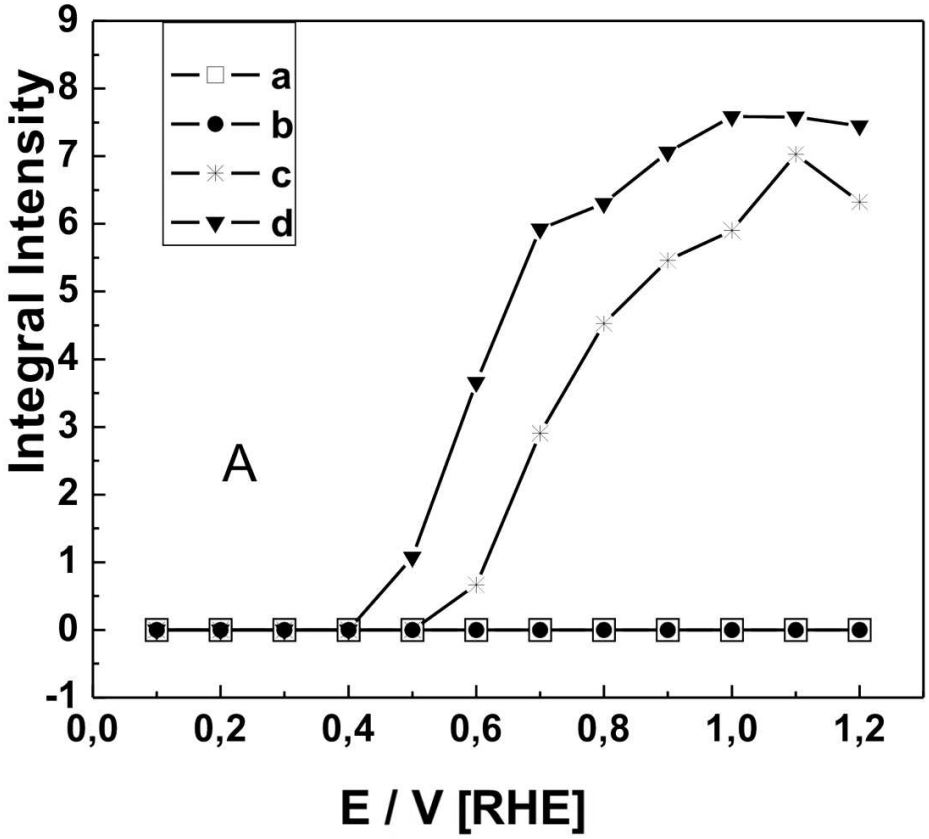

Figure 3. (A) Intensity of the band at 1580 cm-1 as a function of the polarization potential. (a) 0.01 M NaOH + 0.99 M NaClO4 + 1 M EG; (b) 0.1 M NaOH + 0.9 M NaClO4 + 1 M EG; (c) 1 M NaOH + 1 M EG; (d) 2 M NaOH + 1 M EG. (B) Intensity of the band at 1070 cm-1 as a function of the polarization potential. (a) 0.01 M NaOH + 0.99 M NaClO4 + 1 M EG; (b) 0.1 M NaOH + 0.9 M NaClO4 + 1 M EG; (c) 1 M NaOH + 1 M EG; (d) 2 M NaOH + 1 M EG.
74x65mm (400 x 400 DPI)

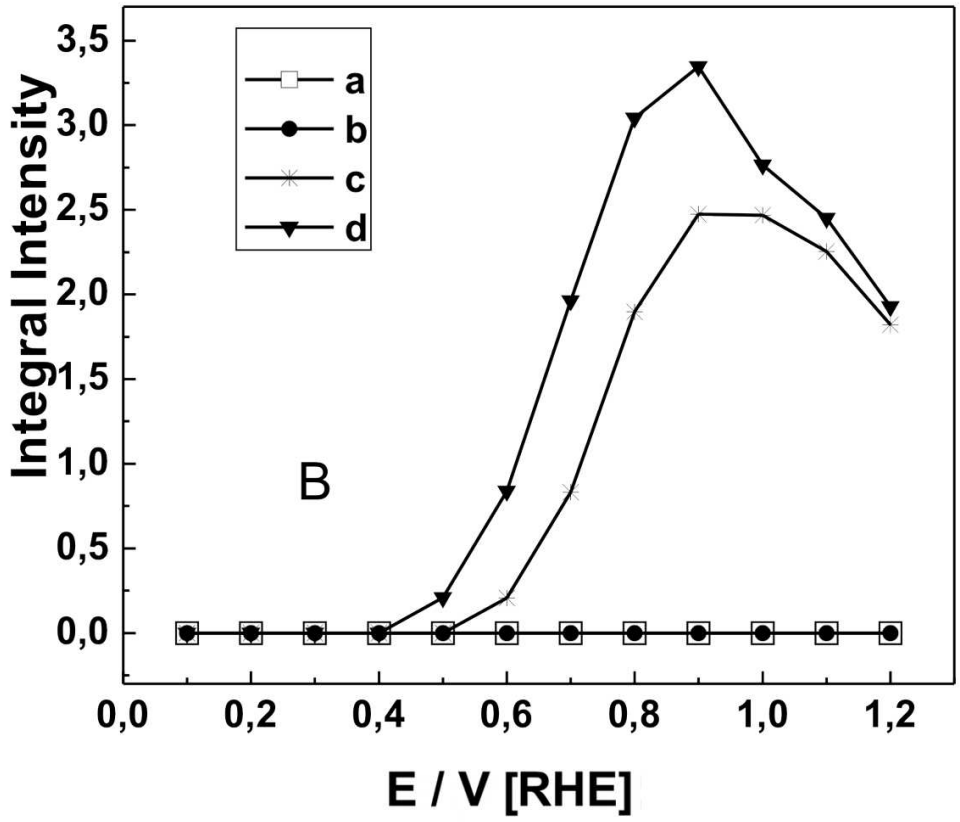

Figure 3. (A) Intensity of the band at 1580 cm-1 as a function of the polarization potential. (a) 0.01 M NaOH + 0.99 M NaClO4 + 1 M EG; (b) 0.1 M NaOH + 0.9 M NaClO4 + 1 M EG; (c) 1 M NaOH + 1 M EG; (d) 2 M NaOH + 1 M EG. (B) Intensity of the band at 1070 cm-1 as a function of the polarization potential. (a) 0.01 M NaOH + 0.99 M NaClO4 + 1 M EG; (b) 0.1 M NaOH + 0.9 M NaClO4 + 1 M EG; (c) 1 M NaOH + 1 M EG; (d) 2 M NaOH + 1 M EG.
74x65mm (400 x 400 DPI)

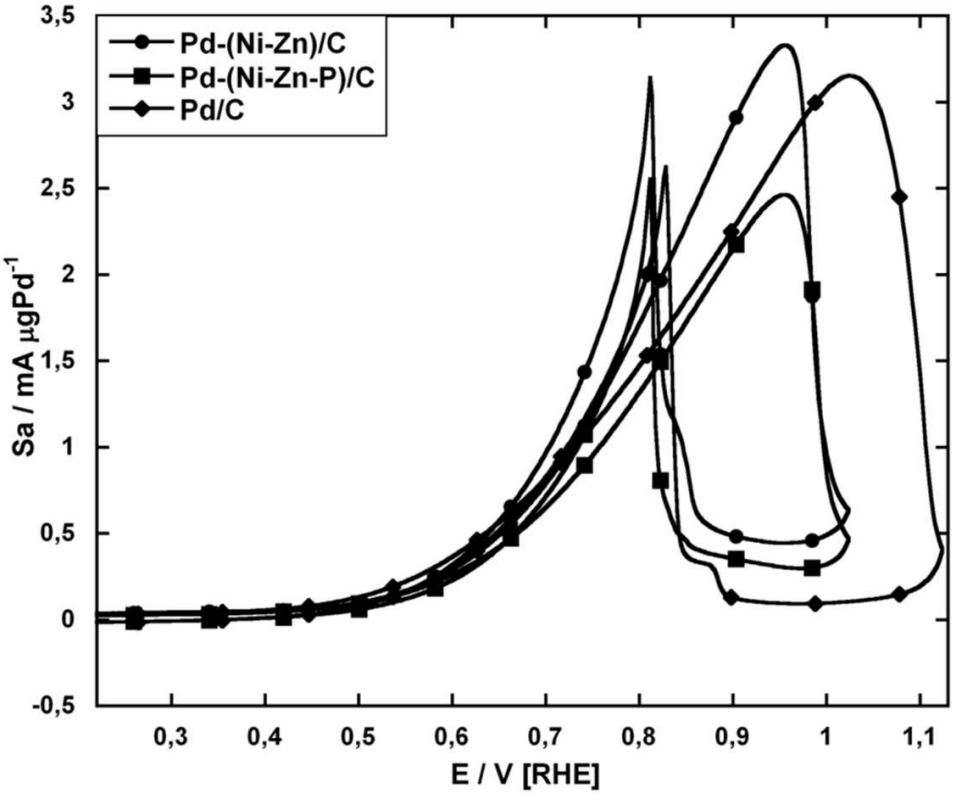

Figure 4. Cyclic voltammograms (at the tenth cycle) of EG oxidation on Pd-(Ni-Zn)/C, Pd-(Ni-Zn-P)/C and Pd/C electrodes in 2 M KOH and 5 wt% EG. Scan rate: 50 mV s-1.
74x65mm (400 x 400 DPI)

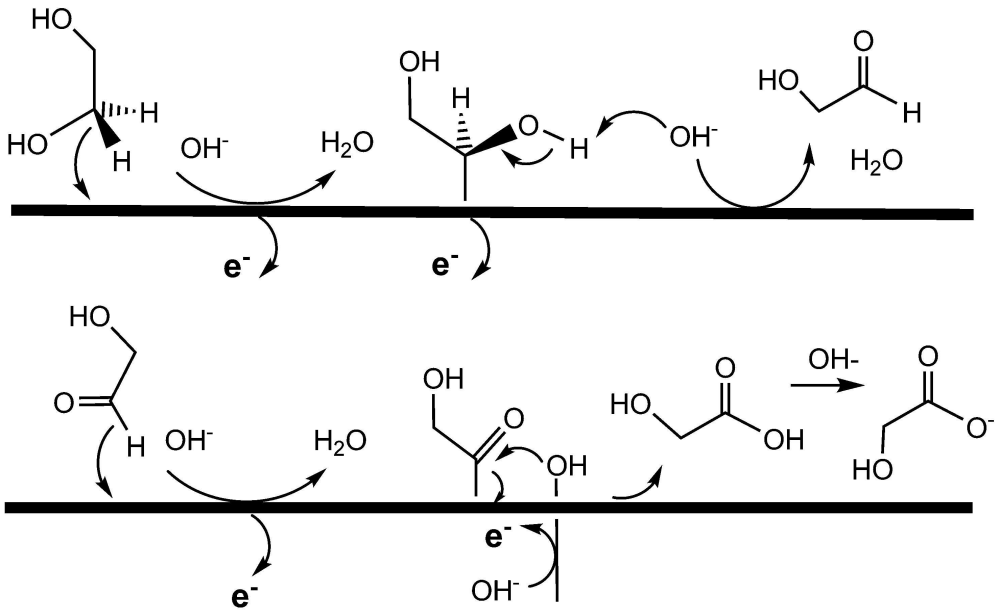

Scheme 1. Proposed mechanism for the electrooxidation of EG to glycolate acid on Pd in alkaline media.
125x77mm (600 x 600 DPI)

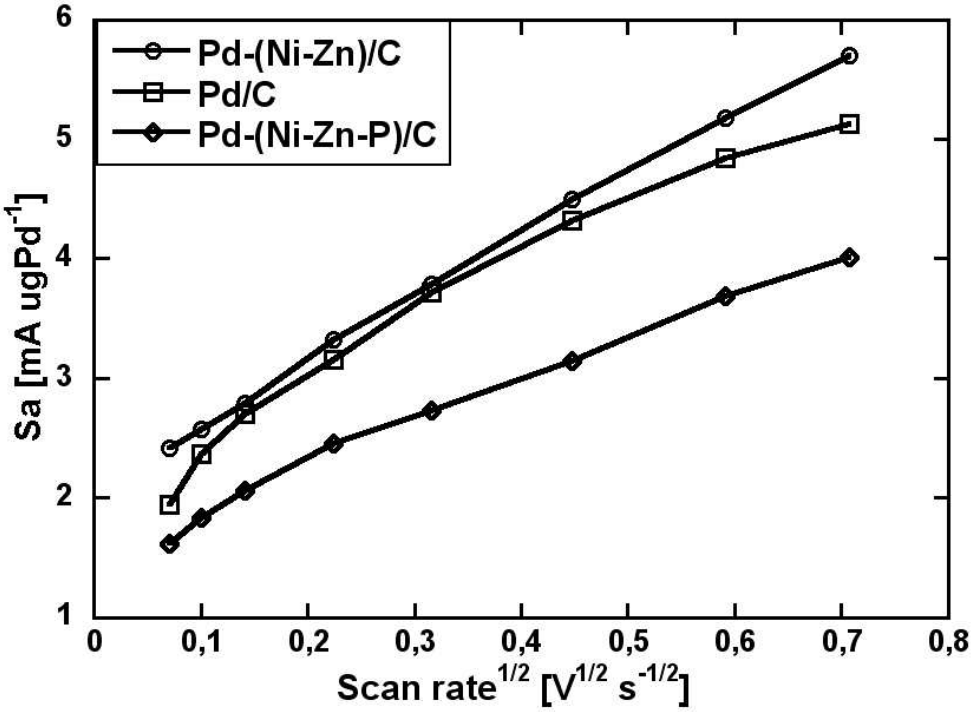

Figure 5. Plots of the anodic peak specific current density against the square-root of the scan rate for the oxidation of EG (5 wt%) on Pd-(Ni-Zn)/C, Pd-(Ni-Zn-P)/C and Pd/C in 2 M KOH.
74x54mm (288 x 288 DPI)

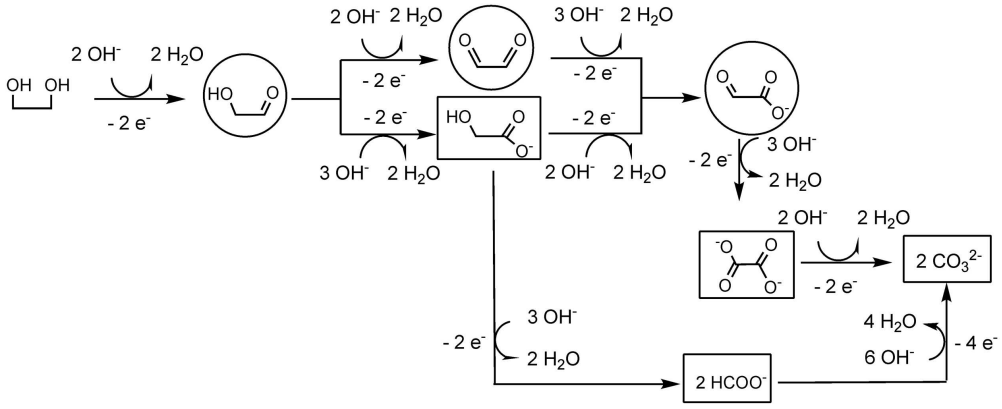

Scheme 2. Overall reaction scheme of EG oxidation on metal electrocatalysyts in alkaline media. Products in boxes have been isolated; products in circles have been detected spectroscopically.
160x65mm (400 x 400 DPI)

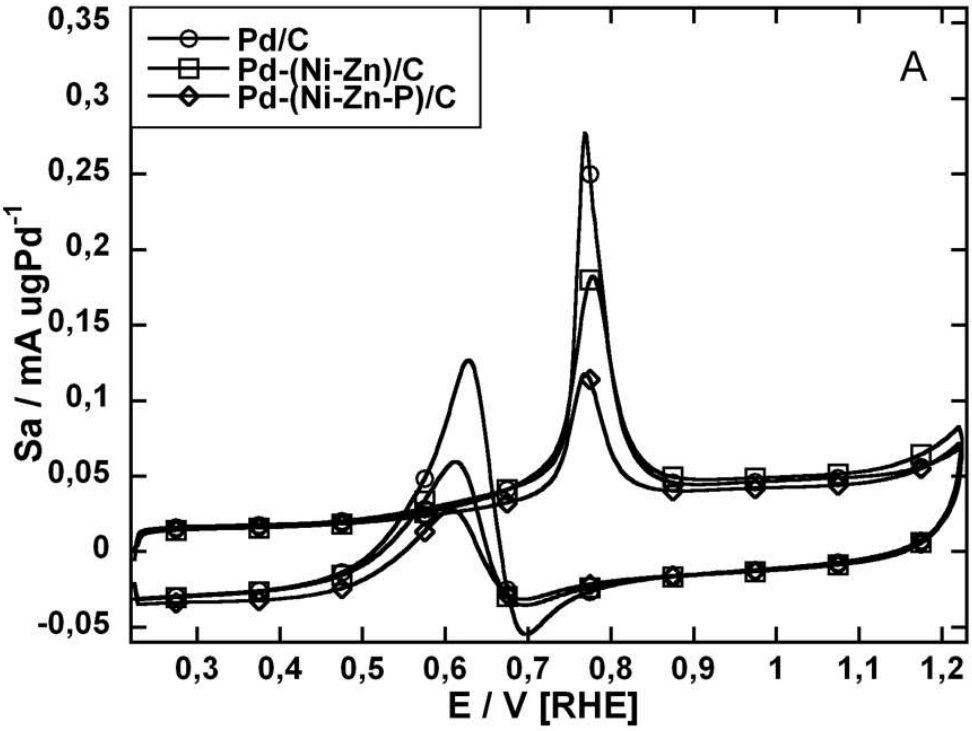

Figure 6. Cyclic voltammograms of (A) glycolic acid (2 wt%) and (B) glyoxylic acid (2 wt%) oxidation on Pd-(Ni-Zn)/C, Pd-(Ni-Zn-P)/C and Pd/C in 2 M KOH. Scan rate: 50 mV s-1.
75x57mm (300 x 300 DPI)

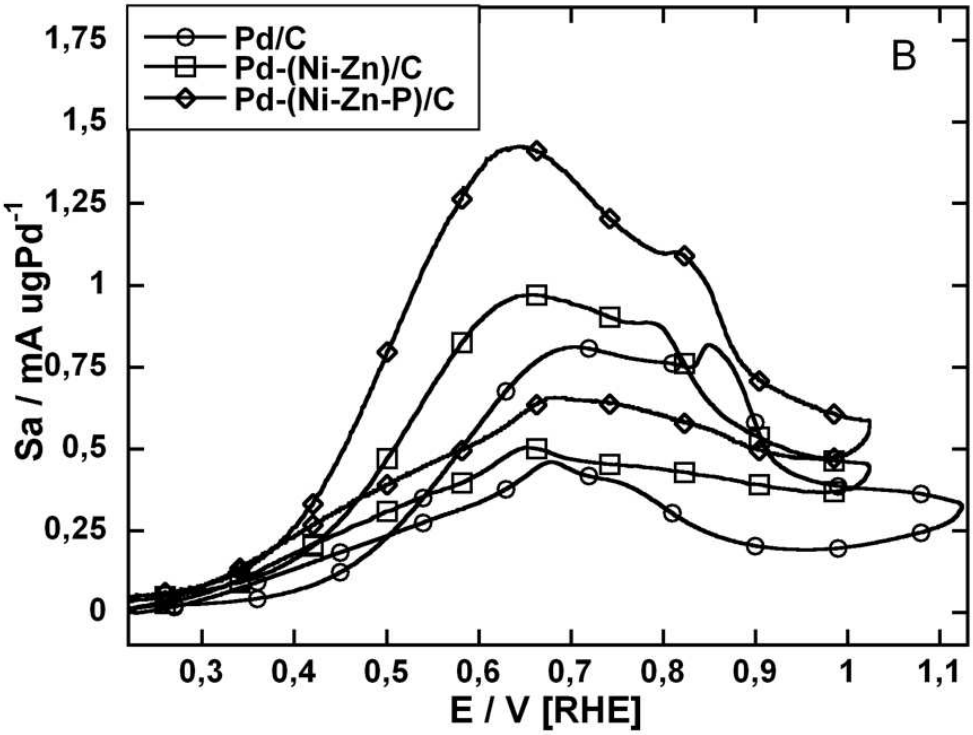

Figure 6. Cyclic voltammograms of (A) glycolic acid (2 wt%) and (B) glyoxylic acid (2 wt%) oxidation on Pd-(Ni-Zn)/C, Pd-(Ni-Zn-P)/C and Pd/C in 2 M KOH. Scan rate: 50 mV s-1.
75x57mm (300 x 300 DPI)

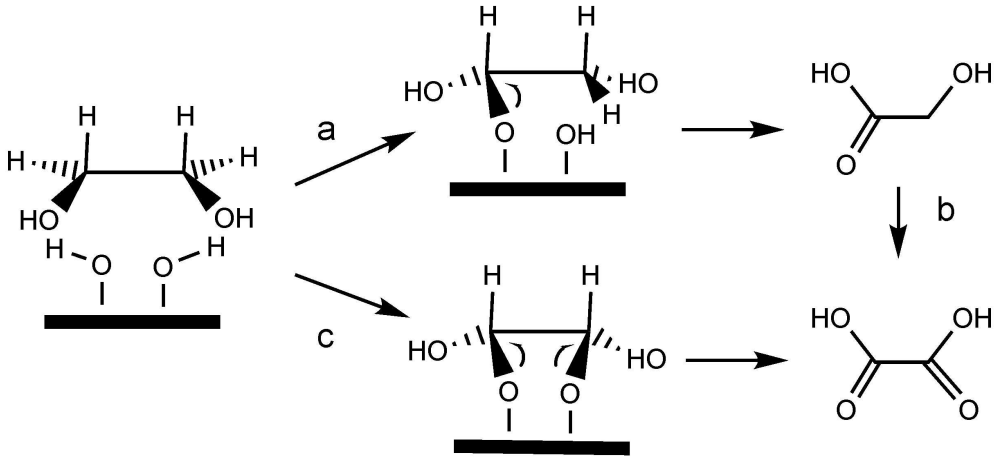

Scheme 3. Direct and sequential routes for the electrooxidation of EG to oxalic acid.
103x48mm (600 x 600 DPI)

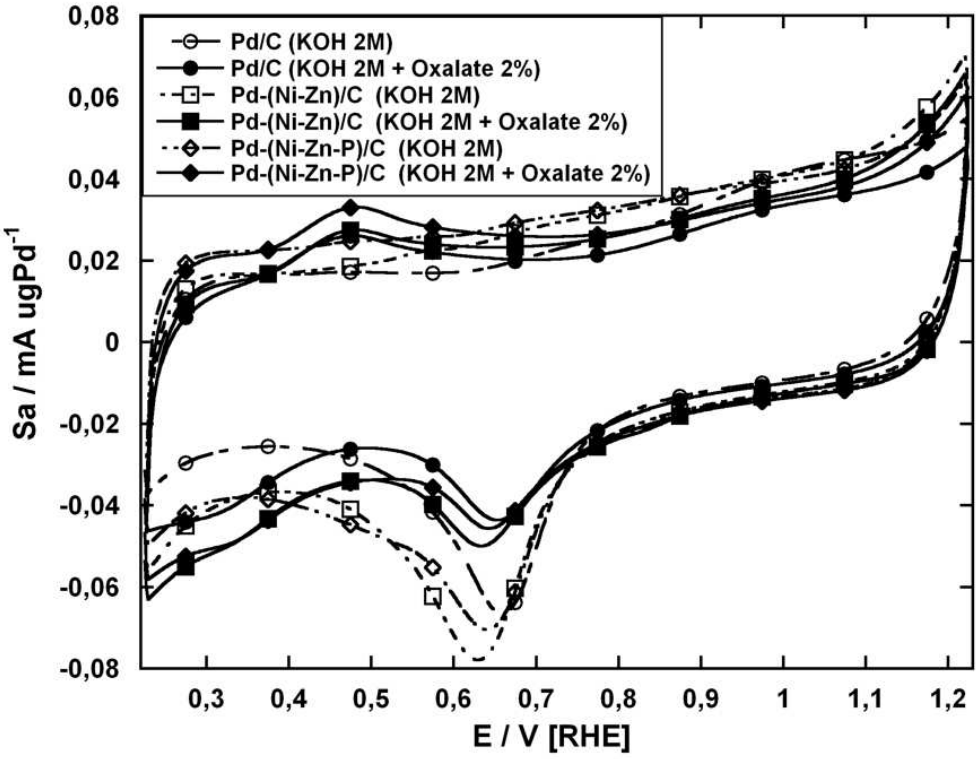

Figure 7. Cyclic voltammograns of Pd-(Ni-Zn)/C, Pd-(Ni-Zn-P)/C and Pd/C in 2 M KOH or in 2 M KOH +2 wt% oxalic acid. Scan rate: 50 mV s-1.
75x57mm (300 x 300 DPI)